Numerical rates for nucleon-nucleon, axion bremsstrahlung

Ralf Peter Brinkmann
Department of Astronomy and Astrophysics, Enrico Fermi Institute, The University of Chicago, Chicago, Illinois 60637-1433
Institut für Theoretische Physik IV, Ruhr-Universität Bochum, 4630 Bochum, Federal Republic of Germany
and NASA/Fermilab Astrophysics Center, Fermi National Accelerator Laboratory, P.O. Box 500, Batavia, Illinois 60510-0500

Michael S. Turner
Department of Astronomy and Astrophysics and Department of Physics, Enrico Fermi Institute, The University of Chicago, Chicago, Illinois 60637-1433
and NASA/Fermilab Astrophysics Center, Fermi National Accelerator Laboratory, P.O. Box 500, Batavia, Illinois 60510-0500
(Received 11 April 1988)

We numerically evaluate the axion emission rate from nucleon-nucleon, axion bremsstrahlung for arbitrary nucleon degeneracy(ies). Our numerical rates agree with analytical results previously derived in the degenerate and nondegenerate limits. While the conditions in the newly born, hot neutron star associated with SN1987A are semidegenerate, the nondegenerate, analytical rate is found to be a very good approximation (accurate to better than a factor of 2), while the degenerate, analytical rate *overestimates* axion emission by a factor of $\sim 20-100$.

INTRODUCTION

To date Peccei-Quinn symmetry provides the most attractive solution to the strong *CP* problem (for discussion of the strong *CP* problem and Peccei-Quinn symmetry see Ref. 1). The axion is the pseudo-Nambu-Goldstone boson associated with the spontaneous breakdown of Peccei-Quinn symmetry. Its mass and couplings are related to the Peccei-Quinn symmetry-breaking scale f_a:

$$m_a \simeq 0.62 \text{ eV}[10^7 \text{ GeV}/(f_a/N)] ,$$

$$g_{ai} \sim m_i/(f_a/N) ,$$

where N is the color anomaly of the Peccei-Quinn symmetry. (Here we have followed the normalization conventions of Ref. 2; for a complete discussion of the axion and its couplings see Refs. 2 and 3.)

Astrophysics and cosmology have placed very stringent limits to the allowed mass of this hypothetical, light pseudoscalar boson (for a review see Ref. 4). Requiring that the cosmological population of coherently produced axions does not contribute too much mass density today leads to the bound[5]

$$m_a \gtrsim 3.6\times 10^{-6} \text{ eV}\gamma^{-0.85}(\Lambda_{\rm QCD}/200 \text{ MeV})^{-0.6} ,$$

where $\Lambda_{\rm QCD}$ is the QCD scale parameter and $\gamma \gtrsim 1$ accounts for any entropy produced in the Universe after axion production: γ=(entropy per comoving volume after/entropy per comoving volume before).

Light axions (if they exist) should be emitted from stars of all varieties (main sequence, red giants, white dwarfs, neutron stars), and should thereby affect stellar evolution. The most stringent stellar emission bound is the recently derived bound based upon axion emission from the newly born, hot neutron star associated with SN1987A (Refs. 6–8). For the conditions that pertain in the core of the hot neutron star just after its formation;[9] $T\sim 30-80$ MeV, $\rho \simeq (6-10)\times 10^{14}$ g cm^{-3}, the dominant emission process is nucleon-nucleon, axion bremsstrahlung (NNAB): $N+N\rightarrow N+N+a$ (N=neutron or proton).

The matrix element for this process, as well as the emission rate in the degenerate (D) limit, have been calculated by Iwamoto.[10] Using the matrix element computed by Iwamoto, the author of Ref. 6 has calculated the emission rate in the nondegenerate (ND) limit. Those two rates for the process $n+n\rightarrow n+n+a$ (n=neutron) are

$$\dot{\epsilon}_a(\text{D}) = 5.3\times 10^{44} \text{ erg cm}^{-3}\text{sec}^{-1} f^4 g_{an}^2 (X_n\rho_{14})^{1/3} T_{\rm MeV}^6 , \quad (1a)$$

$$\dot{\epsilon}_a(\text{ND}) = 1.1\times 10^{47} \text{ erg cm}^{-3}\text{sec}^{-1} f^4 g_{an}^2 (X_n\rho_{14})^{2} T_{\rm MeV}^{3.5} , \quad (1b)$$

where $f\sim 1$ is the pion-nucleon coupling, $g_{an}\sim m/(f_a/N)$ is the axion-neutron coupling, $m\simeq 0.94$ GeV is the nucleon mass, X_n is the mass fraction of neutrons, $\rho_{14}=\rho/10^{14}$ g cm^{-3}, and $T_{\rm MeV}=T/1$ MeV. (For a detailed discussion of the axion-nucleon coupling g_{an} in various axion models, see Refs. 2, 3, 6, and 7. For the moment we will focus on the process $n+n\rightarrow n+n+a$; later we will extend our discussions to all the NNAB processes.) The degenerate (D) and nondegenerate (ND) axion emission rates for $n+n\rightarrow n+n+a$ (or $p+p\rightarrow p+p+a$) are shown in Fig. 1 for $X_n\rho_{14}\simeq 4$, as a function of temperature.

The neutron Fermi momentum $p_F=0.237$ GeV$(X_n\rho_{14})^{1/3}$, so that $p_F^2/2mT \simeq 30(X_n\rho_{14})^{2/3}/T_{\rm MeV} \simeq 75/T_{\rm MeV}$ (for $X_n\rho_{14}\simeq 4$). That is, one would expect the ND rate to be valid for $T \gg 75$ MeV and the D rate to be valid for $T \ll 75$ MeV; the temperatures that pertain just after collapse are $\sim 30-80$ MeV, corresponding to neither strongly ND nor D conditions. The two rates $\dot{\epsilon}_a$(D) and $\dot{\epsilon}_a$(ND) are equal for $T\simeq 20$ MeV: in the D limit ($T \ll 75$ MeV) the ND rate overestimates axion emission, as one would expect since blocking factors are ignored, and in the ND limit ($T \gg 75$ MeV) the D rate overestimates axion emission, as one would also expect since the

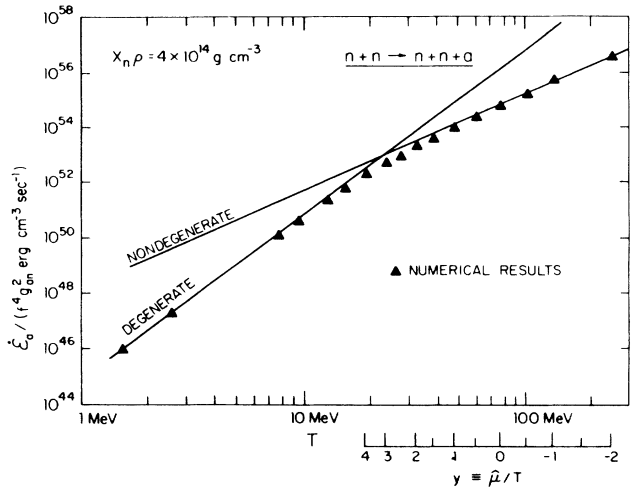

FIG. 1. The axion emission rate from neutron-neutron, axion bremsstrahlung, for $X_n\rho_{14}=4$. Shown are the analytical expressions valid in the D and ND limits, cf. Eqs. (1a) and (1b), and our numerical results which are accurate to better than 1% (indicated by the triangles). The temperature which pertains in the core shortly after collpase is ~ 70 MeV. Also shown is $y\equiv\hat{\mu}/T$ as a function of T.

D rate is more temperature dependent (see Fig. 1).

Which rate is appropriate for SN1987A? Since the two analytic rates cross each other for $T\simeq 20$ MeV (where $p_F^2/2mT\simeq 3.5$) one might naively expect that the ND rate is the better approximation (as we will show, that is in fact the case). The authors of Refs. 7 and 8 use the D rate to compute axion emission from SN1987A, while the author of Ref. 6 uses the ND rate: for $T\simeq 75$ MeV they differ by a factor of $\dot{\epsilon}_a(\mathrm{D})/\dot{\epsilon}_a(\mathrm{ND})\simeq 20$. Since any limit to the axion mass in $\propto \dot{\epsilon}_a^{-1/2}$, this corresponds to a discrepancy of a factor of ~ 5, a significant difference. For the same form of the axion-nucleon coupling, the authors of Ref. 7 derive the bound, $m_a \lesssim 0.9\times10^{-4}$, and the author of Ref. 6, $m_a \lesssim 0.75\times10^{-3}$, a factor of ~ 8 difference, much of which apparently traces to the different axion emission rate used. Since the axion mass bound based upon SN1987A is the most stringent upper bound to the axion mass, we feel it is important to resolve the discrepancy due solely to the axion emission rates.[12] This is the motivation for this work.

In this paper we numerically integrate the axion emission rate for the processes $N+N\rightarrow N+N+a$ ($N=$neutron or proton) for arbitrary degeneracy(ies). Our numerical results are shown in Figs. 1–3 and are compiled in Tables I and II. The numerical results smoothly connect the ND and D limits, and indicate that for the conditions that pertain in the newly born, hot neutron star associated with SN1987A the ND axion emission rate is the better approximation (accurate to better than a factor of 2), with the D rate *overestimating* axion emission by a factor of ~ 10–100. This is our main result. In the Appendix we calculate the matrix element squared for all three NNAB processes, and provide explicit formulas for the total axion emission rate.

AXION EMISSION, ONE CHEMICAL POTENTIAL

To begin we will focus on the process $n+n\rightarrow n+n+a$ (or equivalently, $p+p\rightarrow p+p+a$ or $n+p\rightarrow n+p+a$ with $X_n=X_p$) as there is but one chemical potential; in the next section we extend our discussion to $n+p\rightarrow n+p+a$ and two unequal chemical potentials. The axion emission rate is given by a 15-dimensional phase-space integral:

$$\dot{\epsilon}_a=\int d\Pi_1 d\Pi_2 d\Pi_3 d\Pi_4 d\Pi_a (2\pi)^4 S\,|\mathcal{M}|^2\delta^4(p_1+p_2-p_3-p_4-p_a)E_a f_1 f_2(1-f_3)(1-f_4)\,, \tag{2}$$

where $d\Pi_i=d^3p_i/(2\pi)^3 2E_i$, the labels $i=1$–4 denote the incoming (1,2) and outgoing (3,4) nucleons (at present, neutrons), the label a denotes the axion, the matrix element squared $|\mathcal{M}|^2$ is summed over initial and final spins, and S is the usual symmetry factor for identical particles in the initial and final states: here $S=\frac{1}{4}=\frac{1}{2}\times\frac{1}{2}$. The neutron phase-space distribution functions $f_i=[\exp(E_i/T-\mu/T)+1]^{-1}$. (For the axion masses of interest, $m_a\sim 10^{-3}$ eV, axions simply "free stream" out, and there is no need to take into account reabsorption, or include the $1+f_a$ factor for stimulated emission. For an axion mass $\gtrsim 0.02$ eV, axions become trapped in the core, and like neutrinos are radiated from an "axionsphere."[6] While we will not treat this regime here, we hope to do so in a future publication.) In keeping with the assumptions of previous authors (and for simplicity) we will assume the nucleons are nonrelativistic, i.e., $T/m\ll 1$, and take the matrix element squared to be constant:

$$S\times|\mathcal{M}|^2=\tfrac{1}{4}\times 256 f^2 g_{an}^2 m^2/m_\pi^4\,, \tag{3}$$

where $m_\pi\simeq 135$ MeV is the pion mass and the factor of $S=\frac{1}{4}$ is the usual statistical factor for identical particles in the initial and final states. The matrix element squared is discussed in detail in our Appendix. Two things should be noted. First, $|\mathcal{M}|^2$ is only exactly constant in the limit that $T\gg m_\pi^2/3m\simeq 6$ MeV. For the purpose at hand, where the temperatures are $\gg 6$ MeV this seems like a very adequate approximation, and makes our numerical calculations tractable. Second, our explicit calculation of $|\mathcal{M}|^2$ differs from Iwamoto's calculation[10] of $|\mathcal{M}|^2$ in the degenerate limit by a factor of $(1-\beta/3)$, where β depends upon the degree of degeneracy: $\beta\rightarrow 0$

(degenerate limit); $\beta \to 1.0845$ (nondegenerate limit). For simplicity of comparison and consistency with previous work we will use Iwamoto's value for $|\mathcal{M}|^2$. In the Appendix we will provide our expressions for $|\mathcal{M}|^2$ and for the total axion emission rate based upon those expressions.

In the nonrelativistic (NR), limit, $E_i \simeq m + p_i^2/2m$, and we define the NR chemical potential $\hat{\mu} \equiv \mu - m$. Further, we define the dimensionless quantities

$$y \equiv \hat{\mu}/T, \quad u_i \equiv p_i^2/2mT \ .$$

With these definitions the phase-space occupancy factors f_i are $f_i = 1/(e^{u_i - y}+1)$. The number density (per cm^3) of neutrons (or protons) is then

$$\begin{aligned} n_n &= 2\int_0^\infty \frac{d^3p}{(2\pi)^3} f \\ &= (\sqrt{2}/\pi^2)(mT)^{3/2}\int_0^\infty \frac{u^{1/2}du}{e^{u-y}+1} \\ &= 4.1\times 10^{-6}\ \text{GeV}^3 T_{\text{MeV}}^{3/2} g(y) \ , \end{aligned}$$

where $g(y) \equiv \int_0^\infty u^{1/2}du/(e^{u-y}+1)$. Throughout we use units where $\hbar = c = k_B = 1$, so that 1 GeV$^3 = 1.3\times 10^{41}$ cm^{-3} and GeV$^5 = 3.2\times 10^{62}$ erg cm^{-3} sec^{-1}. We also note that $X_n \rho_{14} \simeq 9.0\times 10^{-3} g(y) T_{\text{MeV}}^{3/2}$. The function $g(y)$ has the following familiar limiting forms:

$$\begin{aligned} g(y) &= \int_0^\infty \frac{u^{1/2}du}{e^{u-y}+1} \\ &\simeq \begin{cases} (\pi^{1/2}/2 \simeq 0.886)e^y, & y \ll -1 \ , \\ \frac{2}{3}y^{3/2}, & y \gg 1 \ . \end{cases} \end{aligned}$$

For intermediate values $g(y)$ is well approximated by its Taylor expansion (to better than 1% for $-1 \lesssim y \lesssim 5$)

$$\begin{aligned} g(y) = 0.678 &+ 0.536y + 0.1685y^2 \\ &+ 0.0175y^3 - 3.24\times 10^{-3} y^4 \ . \end{aligned}$$

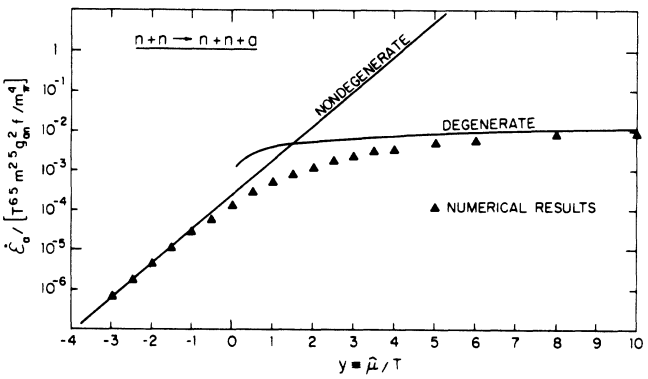

FIG. 2. The axion emission rate from neutron-neutron, axion bremsstrahlung as a function of $y \equiv \hat{\mu}/T$. Shown are the analytical expressions valid in the D and ND limits, cf. Eqs. (5b) and (6b), and the results of our numerical integrations which are accurate to better than 1% (indicated by the triangles).

The neutron Fermi momentum is $p_F \equiv (3\pi^2 n_n)^{1/3}$; in the limit of $y \gg 1$, $p_F^2/2mT \simeq y$; while in the limit of $y \ll -1$, $(p_F^2/2mT) \simeq 1.2\exp(2y/3)$.

It is convenient to define the center-of-mass (c.m.) and relative momenta: $\mathbf{p}_+ \equiv (\mathbf{p}_1 + \mathbf{p}_2)/2$ and $\mathbf{p}_- \equiv (\mathbf{p}_1 - \mathbf{p}_2)/2$, and the momenta of n_3 and n_4 in the c.m. frame: $\mathbf{p}_{3c} = \mathbf{p}_3 - \mathbf{p}_+$ and $\mathbf{p}_{4c} = \mathbf{p}_4 - \mathbf{p}_+$. In the NR limit ($T/m \ll 1$), the outgoing neutrons (n_3 and n_4) carry essentially all of the momentum and the axion momentum can be neglected. Momentum conservation then implies $\mathbf{p}_{4c} = -\mathbf{p}_{3c}$, while energy conservation implies $E_a = p_-^2/m - p_{3c}^2/m$. With these definitions and the aid of the delta function 10 of the 15 integrations can be immediately performed, yielding

$$\begin{aligned} \dot{\epsilon}_a = \frac{S|\mathcal{M}|^2 T^{6.5} m^{0.5}}{2^{3.5}\pi^7} &\int_0^\infty du_+ \int_0^\infty du_- \int_{-1}^1 d\gamma_1 \int_0^{u_-} du_{3c} \int_{-1}^1 d\gamma_c \\ &\times (u_+ u_- u_{3c})^{1/2} (u_- - u_{3c})^2 f_1(u_{1,}y) f_2(u_2,y)[1-f_3(u_3,y)][1-f_4(u_4,y)] \ , \end{aligned} \tag{4}$$

where $u_{1,2} = u_+ + u_- \pm 2(u_+ u_-)^{1/2}\gamma_1$, $u_{3,4} = u_{3c} + u_+ \pm 2(u_{3c}u_+)^{1/2}\gamma_c$, $\gamma_1 = \mathbf{p}_+ \cdot \mathbf{p}_-/|\mathbf{p}_+||\mathbf{p}_-|$, $\gamma_c = \mathbf{p}_+ \cdot \mathbf{p}_{3c}/|\mathbf{p}_+||\mathbf{p}_{3c}|$, and the constant matrix element squared has been taken out of the integral. From this expression for $\dot{\epsilon}_a$ it is immediately clear that the axion emission rate is proportional to $T^{6.5}$ times a function of $y \equiv \hat{\mu}/T$ only. The limiting D and ND rates discussed in the Introduction, cf. Eqs. (1a) and (1b), are of this form, which is reassuring.

At this point it its straightforward to compute the axion emission rate in the ND limit ($y \ll -1$) by neglecting the $1-f_3$, $1-f_4$ "blocking" factors and setting $f_i = e^{y-u_i}$. The integrand becomes independent of γ_c and γ_1, and the γ_c, γ_1 integrals can be done trivially. The other integrations can also be done, giving

$$\dot{\epsilon}_a(\text{ND}) = \frac{1}{4\times 35\pi^{6.5}} S|\mathcal{M}|^2 m^{0.5} T^{6.5} e^{2y} \tag{5a}$$

$$= 2.68\times 10^{-4} e^{2y} m^{2.5} T^{6.5} m_\pi^{-4} g_{an}^2 f^4 \ , \tag{5b}$$

$$= 1.1\times 10^{47}\ \text{erg cm}^{-3}\text{sec}^{-1} f^4 g_{an}^2 (X_n \rho_{14})^2 T_{\text{MeV}}^{3.5} \ , \tag{5c}$$

where Eq. (5b) follows from (5a) by substituting $S|\mathcal{M}|^2 = 64 g_{an}^2 f^4 m^2/m_\pi^4$, and Eq. (5c) from (5b) by substituting $e^y \simeq 125(X_n\rho_{14})T_{\text{MeV}}^{-3/2}$ (valid for $y \ll -1$). This agrees with the result previously derived in Ref. 6 (see also Refs. 11 and

13).

The D limit ($y \gg 1$) has been derived by Iwamoto;[10] he obtains

$$\dot{\epsilon}_a(\mathrm{D}) = \frac{31\sqrt{2}}{3780\pi} m^{2.5} T^{6.5} m_\pi^{-4} g_{an}^2 f^4 y^{1/2} \tag{6a}$$

$$= 3.69\times 10^{-3} y^{1/2} m^{2.5} T^{6.5} m_\pi^{-4} g_{an}^2 f^4 \tag{6b}$$

$$= 5.3\times 10^{44}\ \mathrm{erg\,cm^{-3}sec^{-1}}\, f^4 g_{an}^2 (X_n \rho_{14})^{1/3} T_{\mathrm{MeV}}^6 \ . \tag{6c}$$

By first performing the γ_1 and γ_c integrations (see below), and then expanding the rapidly varying parts of the integrand in a series of step functions, delta functions, and their derivatives, with some effort we have verified Iwamoto's result for the degenerate limit. In addition we have determined that the next term in the expansion is of order $O(y^{-1})y^{1/2}$. The ND and D limit axion emission rates are shown in both Fig. 1 (as a function of T) and in Fig. 2 (as a function of $y \equiv \hat{\mu}/T$).

Returning to the general case (arbitrary y), both the γ_1 and γ_c integrations can be performed, and with the further substitutions $v \equiv u_{3c}/u_-$ and $q_\pm = e^{-u_\pm}$, $\dot{\epsilon}_a$ can be expressed as a three-dimensional integral:

$$\dot{\epsilon}_a = \frac{S\,|\mathcal{M}|^2 m^{0.5} T^{6.5}}{2^{5.5}\pi^7} \int_0^1 dq_+ \int_0^1 dq_- \int_0^1 dv\, u_+^{-1/2} u_-^3 (1-v)^2 q_+ q_- (e^{-2y} - q_+^2 q_-^2)^{-1}$$
$$\times [1-\exp(2y - 2vu_- - 2u_+)]^{-1} \ln\left[\frac{\cosh^2[(u_+^{1/2}+u_-^{1/2})^2/2 - y/2]}{\cosh^2[(u_+^{1/2}-u_-^{1/2})^2/2 - y/2]}\right] \ln\left[\frac{\cosh^2\{[(vu_-)^{1/2}+u_+^{1/2}]^2/2 - y/2\}}{\cosh^2\{[(vu_-)^{1/2}-u_+^{1/2}]^2/2 - y/2\}}\right] \tag{7a}$$

$$\equiv S\,|\mathcal{M}|^2 m^{0.5} T^{6.5} I(y) \ . \tag{7b}$$

This three-dimensional integral must be evaluated numerically. We have used two different numerical techniques to evaluate this integral: Monte Carlo integration and direct integration. For the Monte Carlo technique, the integrand was evaluated at 10^6 randomly chosen points in the domain of integration $q_1, q_2, v \in [0,1]$, and the integral was taken to be the average value of the integrand times the volume of the domain of integration ($=1$). To estimate the error we grouped the 10^6 points into 10 subsamples of 10^5 points each, and computed the individual means of the integrand, and then took the variance of the 10 means. The estimated errors for the Monte Carlo method were typically $\lesssim 10\%$. Be-

TABLE I. Axion emission rate $\dot{\epsilon}_a$ (for $n+n \to n+n+a$): analytical results and numerical results. All numerical results are accurate to better than 1%. Rates are given in units of $T^{6.5} m^{2.5} g_{an}^2 f^4 / m_\pi^4$. The integral $I(y)$, defined in Eq. (7), is equal to the numerical results given here divided by 64.

$y \equiv \hat{\mu}/T$	Numerical	Nondegenerate	Degenerate
−10.0	5.53×10^{-13}	5.52×10^{-13}	
−4.0	8.85×10^{-8}	8.99×10^{-8}	
−3.5	2.38×10^{-7}	2.44×10^{-7}	
−3.0	6.36×10^{-7}	6.64×10^{-7}	
−2.5	1.68×10^{-6}	1.81×10^{-6}	
−2.0	4.36×10^{-6}	4.91×10^{-6}	
−1.5	1.10×10^{-5}	1.33×10^{-5}	
−1.0	2.68×10^{-5}	3.63×10^{-5}	
−0.5	6.17×10^{-5}	9.86×10^{-5}	
0	1.32×10^{-4}	2.68×10^{-4}	0
0.5	2.61×10^{-4}	7.28×10^{-4}	2.61×10^{-3}
1.0	4.72×10^{-4}	1.98×10^{-3}	3.69×10^{-3}
1.5	7.79×10^{-4}	5.38×10^{-3}	4.52×10^{-3}
2.0	1.18×10^{-3}	1.46×10^{-2}	5.22×10^{-3}
2.5	1.67×10^{-3}	3.98×10^{-2}	5.83×10^{-3}
3.0	2.22×10^{-3}	1.08×10^{-1}	6.39×10^{-3}
3.5	2.82×10^{-3}		6.90×10^{-3}
4.0	3.43×10^{-3}		7.38×10^{-3}
5.0	4.64×10^{-3}		8.25×10^{-3}
6.0	5.77×10^{-3}		9.04×10^{-3}
8.0	7.75×10^{-3}		1.04×10^{-2}
10.0	9.37×10^{-3}		1.17×10^{-2}
50.0	2.52×10^{-2}		2.61×10^{-2}

cause of the severe effects of degeneracy for $y \gtrsim 5$, the integrand becomes strongly peaked, and the Monte Carlo technique becomes unreliable. And for this reason we also used a direct technique to numerically integrate Eq. (7). By a judicious series of transformations the integrand can be made very smooth, making direct numerical integration both accurate and fast. The estimated accuracy for all our direct integrations is better than 1%. Our numerical results are shown in Figs. 1 and 2 and compiled in Table I. The following expression is a closed form fit to $I(y)$ which for all values of y is accurate to better than 10%:

$$I_{\rm fit}(y)=[1.79\times10^5 e^{-y}+2.39\times10^5 e^{-2y}+1.73\times10^4(1+|y|)^{-1/2} +6.92\times10^4(1+|y|)^{-3/2}+1.73\times10^4(1+|y|)^{-5/2}]^{-1} .$$

Our chosen range of y spans $y=-10\rightarrow50$. From Fig. 2 and Table I it is clear that the numerical results smoothly join on to the asymptotic limits (D,ND). The approach to the ND limit is much more rapid than the approach to the D limit, which is easy to understand. In the ND limit the expansion parameter is e^y, while in the D limit the expansion is in powers of y^{-1}. From Fig. 1 it is also clear that the ND, analytic rate provides a very good approximation to the actual rate for $p_F^2/2mT \lesssim 3$, or $T \gtrsim 30$ MeV for $X_n\rho_{14}=4$.

TWO CHEMICAL POTENTIALS

To this point we have assumed that the chemical potentials for all four nucleons are equal. For the processes $n_1+n_2\rightarrow n_3+n_4+a$ and $p_1+p_2+p_3+p_4+a$ this is of course true. However, if one wishes to consider the process $n_1+p_2\rightarrow n_3+p_4+a$ this assumption is only valid if $X_n=X_p$. It is straightforward to relax the assumption of equal chemical potentials by defining separate neutron ($y_1\equiv\hat{\mu}_n/T$) and proton ($y_2\equiv\hat{\mu}_p/T$) chemical potentials. In this case the analogue of Eq. (7) is

$$\dot{\epsilon}_a=\frac{S\,|\mathcal{M}|^2 m^{0.5}T^{6.5}}{2^{5.5}\pi^7}\int_0^1 dq_+\int_0^1 dq_-\int_0^1 dv\, u_+^{-1/2}u_-^3(1-v)^2 q_+q_-(e^{-y_1}e^{-y_2}-q_+^2q_-^2)^{-1} \times[1-\exp(y_1+y_2-2vu_- -2u_+)]^{-1}\ln\left\{\frac{\{1+\exp[(u_-^{1/2}+u_+^{1/2})^2-y_1]\}\{1+\exp[y_2-(u_-^{1/2}+u_+^{1/2})^2]\}}{\{1+\exp[(u_-^{1/2}-u_+^{1/2})^2-y_1]\}\{1+\exp[y_2-(u_-^{1/2}-u_+^{1/2})^2]\}}\right\} \times\ln\left\{\frac{(1+\exp\{[(vu_-)^{1/2}+u_+^{1/2}]^2-y_1\})(1+\exp\{y_2-[(vu_-)^{1/2}+u_+^{1/2}]^2\})}{(1+\exp\{[(vu_-)^{1/2}-u_+^{1/2}]^2-y_1\})(1+\exp\{y_2-[(vu_-)^{1/2}-u_+^{1/2}]^2\})}\right\} \quad (8a)$$

$$\equiv S\,|\mathcal{M}|^2 m^{0.5}T^{6.5}I(y_1,y_2) . \quad (8b)$$

In the limit that $y\equiv y_1=y_2$ this expression reduces to Eq. (7), and $I(y,y)=I(y)$. Also note that $\dot{\epsilon}_a$ is again proportional to $T^{6.5}$ times a function of y_1 and y_2 alone. As before, the ND limit ($y_1,y_2\ll-1$) is straightforward to obtain

$$\dot{\epsilon}_a({\rm ND})=\frac{1}{4\times35\pi^{6.5}}S\,|\mathcal{M}|^2 m^{0.5}T^{6.5}e^{y_1+y_2} \quad (9a)$$

$$=4.4\times10^{47}\ {\rm erg\,cm^{-3}sec^{-1}}f^4 g_{aN}^2 X_n X_p \rho_{14}^2 T_{\rm MeV}^{3.5} , \quad (9b)$$

where Eq. (9b) follows by substituting $S\,|\mathcal{M}|^2=256m^2g_{aN}^2f^4/m_\pi^4$ (for this process $S=1$ as there are no identical particles in the initial or final states), and g_{aN} is the effective axion nucleon coupling for $n+p\rightarrow n+p+a$ (see Appendix). With some effort, by expanding the integrand as before one obtains the following expression in the D limit ($y_1,y_2\gg1$):

$$\dot{\epsilon}_a(D)=\frac{31\sqrt{2}}{945\pi}m^{2.5}T^{6.5}m_\pi^{-4}g_{aN}^2f^4\bar{y}^{1/2}(1-\Delta y/2\bar{y}) \quad (10a)$$

$$=2.1\times10^{45}\ {\rm erg\,cm^{-3}sec^{-1}}g_{aN}^2f^4\rho_{14}^{1/3}T_{\rm MeV}^6\left\{\frac{X_n^{2/3}+X_p^{2/3}}{2}\right\}^{1/2}(1-\Delta y/2\bar{y}) , \quad (10b)$$

where $\bar{y}=(y_1+y_2)/2$ and $\Delta y=|y_1-y_2|/2$.

Finally, in the limit that $y_1\ll-1$ and $y_2\gg1$ (one degenerate and one nondegenerate species) with a similar amount of effort we find that

$$\dot{\epsilon}_a({\rm D,ND})=\frac{1}{2^{1.5}\pi^{6.5}}m^{2.5}T^{6.5}m_\pi^{-4}g_{aN}^2f^4e^{y_1}\int_0^\infty dw/w^2\int_0^\infty z^2dz\,\ln(1+w)\ln(1+we^{-z}) \quad (11a)$$

$$=5.43\times10^{-3}m^{2.5}T^{6.5}m_\pi^{-4}g_{aN}^2f^4e^{y_1} \quad (11b)$$

$$=1.8\times10^{46}\ 1.8\times10^{46}\ {\rm erg\,cm^{-3}sec^{-1}}g_{aN}^2f^4X_1\rho_{14}T_{\rm MeV}^5 . \quad (11c)$$

We have numerically evaluated $I(y_1,y_2)$ for $y_1,y_2\in[-10,10]$ using the same direct integration technique as before.

Our results, all accurate to better than 1%, are compiled in Table II. These results agree with the analytic expressions derived above in the appropriate limits. The grid of 231 values in Table II can be used to interpolate for all intermediate values. For a point $(\bar{y},\Delta y)$ in between grid points $A=(\bar{y}_i,\Delta y_i)$, $B=(\bar{y}_i,\Delta y_{ii})$, $C=(\bar{y}_{ii},\Delta y_i)$, $D=(\bar{y}_{ii},\Delta y_{ii})$, the double-logarithmic linear interpolation

$$\ln I(\bar{y},\Delta y)\simeq\left[\frac{\bar{y}-\bar{y}_i}{\bar{y}_{ii}-\bar{y}_i}\right]\left[\left[\frac{\Delta y-\Delta y_i}{\Delta y_{ii}-\Delta y_i}\right]\ln I(\bar{y}_i,\Delta y_i)+\left[\frac{\Delta y_{ii}-\Delta y}{\Delta y_{ii}-\Delta y_i}\right]\ln I(\bar{y}_i,\Delta y_{ii})\right]$$
$$+\left[\frac{\bar{y}_{ii}-\bar{y}}{\bar{y}_{ii}-\bar{y}_i}\right]\left[\left[\frac{\Delta y-\Delta y_i}{\Delta y_{ii}-\Delta y_i}\right]\ln I(\bar{y}_{ii},\Delta y_i)+\left[\frac{\Delta y_{ii}-\Delta y}{\Delta y_{ii}-\Delta y_i}\right]\ln I(\bar{y}_{ii},\Delta y_{ii})\right]$$

provides a value for $I(\bar{y},\Delta y)$ which is accurate to better than 5%.

In addition, the following is a closed form fit to $I(y_1,y_2)$ which is accurate to better than 25% for all values of y_1,y_2 (and typically, better than 10%),

$$I_{\rm fit}(y_1,y_2)=[2.39\times10^5(e^{-y_1-y_2}+0.25e^{-y_1}+0.25e^{-y_2})+1.73\times10^4(1+|\bar{y}|)^{-1/2}$$
$$+6.92\times10^4(1+|\bar{y}|)^{-3/2}+1.73\times10^4(1+|\bar{y}|)^{-5/2}]^{-1}\ .$$

To illustrate our results we have computed $\dot{\epsilon}_a$ for $\rho_{14}=8$ as a function of temperature for two sets of abundances: (i) $X_n=0.9$, $X_p=0.1$ and (ii) $X_n=0.7$, $X_p=0.3$. The case $X_n=X_p=0.5$ has already been done, since in this instance $y_1=y_2$ (see Fig. 1). The results for these two cases are shown in Fig. 3, along with the analytic rates for the degenerate and nondegenerate limits [for simplicity, the $(1-\Delta y/2\bar{y})$ factor has not been included for the degenerate limit]. Again, it is clear that for the conditions that pertain in the postcollapse core the nondegenerate rate is a very good approximation, overestimating $\dot{\epsilon}_a$ by at most a factor of 2, while the degenerate rate can overestimate $\dot{\epsilon}_a$ by as much as a factor of 100.

DISCUSSION AND CONCLUDING REMARKS

We have numerically calculated the axion emission rate from nucleon-nucleon, axion bremsstrahlung for arbitrary neutron and proton degeneracy using both Monte Carlo and direct numerical-integration techniques. Our numerical results agree with the analytical results previously obtained in the D ($y\gg1$) and ND ($y\ll-1$) limits,[6,10] and with the analytic expressions we have derived in the various limiting regimes with two chemical potentials. Also, we have explicitly evaluated the matrix element squared for all three processes. Our expression for $|\mathcal{M}|^2$ agrees with Iwamoto's result[10] for $|\mathcal{M}|^2$ (for the process $n+n\rightarrow n+n+a$) in the degenerate limit. The total axion emission rate is given in the Appendix, cf. Eq. (A1).

Somewhat surprisingly, the transition from the D regime to the ND regime occurs for $p_F^2/2mT\sim3.5$ (rather than ~1). For $p_F^2/2mT\lesssim3$, the nondegenerate rate provides a reasonable approximation to the actual axion emission rate. In the nondegenerate regime convergence to the ND rate is rapid. The degenerate regime is rather more complicated. The leading-order term in the degenerate regime expansion varies as the square root of the average chemical potential, and if the two chemical potentials are quite different (as in the case for $X_n=0.9$ and $X_p=0.1$) this can be quite a poor approximation. The convergence to the D limit is quite slow because the expansion is in powers of y^{-1}, and for two chemical potentials because of the additional exacerbating effect of unequal chemical potentials. The slow approach to the degenerate limit is clearly illustrated in Figs. 1–3.

Our motivation for this work was to accurately calculate axion emission from the newly born, hot neutron star associated with SN1987A, where the conditions are that of intermediate degeneracy. From Figs. 1 and 3 it is clear that in the pertinent regime ($\rho_{14}\simeq8$, $T\sim70$ MeV), the ND rate is a good approximation (overestimating the true emission rate by at most a factor of 2), and that the D rate is a poor approximation (overestimating the true emission rate by a factor of ~20–100). Since any axion mass limits which are derived scale as the axion emission rate to the $-\frac{1}{2}$ power, mass limits derived using the D

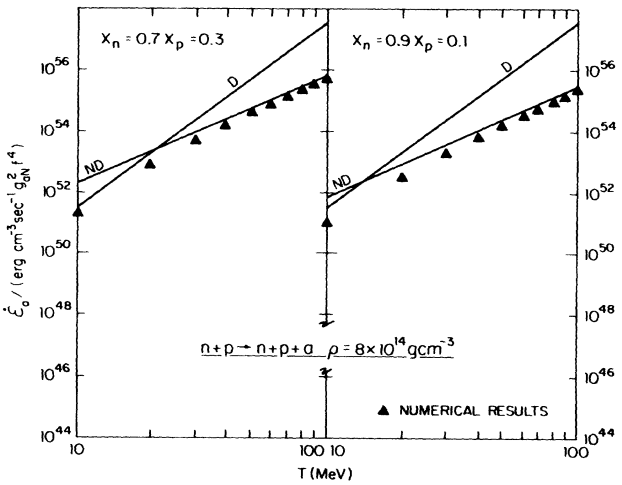

FIG. 3. The axion emission rates from neutron-proton, axion bremsstrahlung, for $\rho=8\times10^{14}\,\mathrm{g\,cm^{-3}}$, and the compositions: $X_n=0.9$, $X_p=0.1$, and $X_n=0.7$, $X_p=0.3$. (Note, Fig. 1 applies to the intermediate case $X_n=X_p=0.5$.) Shown are the analytic expressions valid in the degenerate and nondegenerate limits, as well as our numerical results which are accurate to 1% (indicated by the triangles). [For simplicity the $(1-\Delta y/2\bar{y})$ factor has not been included in the degenerate rate.]

TABLE II. Axion emission rate $\dot{\epsilon}_a$ (from $n+p \rightarrow n+p+a$): numerical results. All rates are accurate to better than 1% and are given in units of $4T^{6.5}m^{2.5}g_{aN}^2 f^4/m_\pi^4$. The quantities $\bar{y}$ and Δy are related to y_1 and y_2 by $\bar{y}=(y_1+y_2)/2$, $\Delta y = |y_1-y_2|/2$. The integral $I(y_1,y_2)$, defined in Eq. (8), is equal to the numerical results given here divided by 64.

$\bar{y}$ \ Δy	0	1	2	3	4	5	6	7	8	9	10
−10	5.53×10^{-13}	5.53×10^{-13}	5.53×10^{-13}	5.53×10^{-13}	5.53×10^{-13}	5.52×10^{-13}	5.49×10^{-13}	5.41×10^{-13}	5.21×10^{-13}	4.75×10^{-13}	3.88×10^{-13}
−9	4.09×10^{-12}	4.09×10^{-12}	4.09×10^{-12}	4.08×10^{-12}	4.08×10^{-12}	4.05×10^{-12}	4.00×10^{-12}	3.85×10^{-12}	3.51×10^{-12}	2.87×10^{-12}	1.98×10^{-12}
−8	3.02×10^{-11}	3.02×10^{-11}	3.02×10^{-11}	3.01×10^{-11}	3.00×10^{-11}	2.95×10^{-11}	2.84×10^{-11}	2.59×10^{-11}	2.12×10^{-11}	1.46×10^{-11}	8.41×10^{-12}
−7	2.23×10^{-10}	2.23×10^{-10}	2.23×10^{-10}	2.21×10^{-10}	2.18×10^{-10}	2.10×10^{-10}	1.92×10^{-10}	1.57×10^{-10}	1.08×10^{-10}	6.21×10^{-11}	3.06×10^{-11}
−6	1.65×10^{-9}	1.64×10^{-9}	1.64×10^{-9}	1.61×10^{-9}	1.55×10^{-9}	1.42×10^{-9}	1.16×10^{-9}	7.99×10^{-10}	4.59×10^{-10}	2.26×10^{-10}	1.00×10^{-10}
−5	1.21×10^{-8}	1.21×10^{-8}	1.19×10^{-8}	1.15×10^{-8}	1.05×10^{-8}	8.54×10^{-9}	5.90×10^{-9}	3.39×10^{-9}	1.67×10^{-9}	7.39×10^{-10}	3.05×10^{-10}
−4	8.86×10^{-8}	8.78×10^{-8}	8.47×10^{-8}	7.73×10^{-8}	6.31×10^{-8}	4.36×10^{-8}	2.51×10^{-8}	1.23×10^{-8}	5.46×10^{-9}	2.25×10^{-9}	8.91×10^{-10}
−3	6.36×10^{-7}	6.21×10^{-7}	5.69×10^{-7}	4.66×10^{-7}	3.22×10^{-7}	1.85×10^{-7}	9.12×10^{-8}	4.03×10^{-8}	1.66×10^{-8}	6.58×10^{-9}	2.54×10^{-9}
−2	4.36×10^{-6}	4.13×10^{-6}	3.42×10^{-6}	2.37×10^{-6}	1.37×10^{-6}	6.74×10^{-7}	2.98×10^{-7}	1.23×10^{-7}	4.86×10^{-8}	1.88×10^{-8}	7.12×10^{-9}
−1	2.68×10^{-5}	2.40×10^{-5}	1.72×10^{-5}	1.00×10^{-5}	4.69×10^{-6}	2.20×10^{-6}	9.08×10^{-7}	3.59×10^{-7}	1.39×10^{-7}	5.26×10^{-8}	1.98×10^{-8}
0	1.32×10^{-4}	1.12×10^{-4}	7.05×10^{-5}	3.60×10^{-5}	1.61×10^{-5}	6.69×10^{-6}	2.65×10^{-6}	1.02×10^{-6}	3.89×10^{-7}	1.46×10^{-7}	5.47×10^{-8}
1	4.72×10^{-4}	3.92×10^{-4}	2.35×10^{-4}	1.13×10^{-4}	4.85×10^{-5}	1.95×10^{-5}	7.54×10^{-6}	2.87×10^{-6}	1.08×10^{-6}	4.04×10^{-7}	1.50×10^{-7}
2	1.18×10^{-3}	1.01×10^{-3}	6.35×10^{-4}	3.17×10^{-4}	1.37×10^{-4}	5.47×10^{-5}	2.11×10^{-5}	7.96×10^{-6}	2.98×10^{-6}	1.11×10^{-6}	4.13×10^{-7}
3	2.22×10^{-3}	1.97×10^{-3}	1.38×10^{-3}	7.68×10^{-4}	3.58×10^{-4}	1.48×10^{-4}	5.77×10^{-5}	2.19×10^{-5}	8.19×10^{-6}	3.05×10^{-6}	1.13×10^{-6}
4	3.43×10^{-3}	3.14×10^{-3}	2.41×10^{-3}	1.55×10^{-3}	8.29×10^{-4}	3.77×10^{-4}	1.54×10^{-4}	5.94×10^{-5}	2.24×10^{-5}	8.34×10^{-6}	3.09×10^{-6}
5	4.64×10^{-3}	4.35×10^{-3}	3.60×10^{-3}	2.61×10^{-3}	1.63×10^{-3}	8.60×10^{-4}	3.88×10^{-4}	1.57×10^{-4}	6.04×10^{-5}	2.27×10^{-5}	8.44×10^{-6}
6	5.77×10^{-3}	5.50×10^{-3}	4.79×10^{-3}	3.80×10^{-3}	2.70×10^{-3}	1.67×10^{-3}	8.77×10^{-4}	3.94×10^{-4}	1.60×10^{-4}	6.12×10^{-5}	2.29×10^{-5}
7	6.81×10^{-3}	6.56×10^{-3}	5.90×10^{-3}	4.97×10^{-3}	3.88×10^{-3}	2.75×10^{-3}	1.70×10^{-3}	8.89×10^{-4}	3.99×10^{-4}	1.61×10^{-4}	6.18×10^{-5}
8	7.75×10^{-3}	7.52×10^{-3}	6.92×10^{-3}	6.06×10^{-3}	5.05×10^{-3}	3.93×10^{-3}	2.78×10^{-3}	1.72×10^{-3}	8.98×10^{-4}	4.02×10^{-4}	1.63×10^{-4}
9	8.60×10^{-3}	8.39×10^{-3}	7.84×10^{-3}	7.06×10^{-3}	6.14×10^{-3}	5.10×10^{-3}	3.96×10^{-3}	2.80×10^{-3}	1.73×10^{-3}	9.04×10^{-4}	4.05×10^{-4}
10	9.37×10^{-3}	9.18×10^{-3}	8.68×10^{-3}	7.97×10^{-3}	7.13×10^{-3}	6.18×10^{-3}	5.13×10^{-3}	3.99×10^{-3}	2.82×10^{-3}	1.74×10^{-3}	9.09×10^{-4}

axion emission rate should be scaled *upward* by a factor of $\sim 5-10$. Applying such a factor to the limit derived in Ref. 7 (where the D rate was used), brings this limit into better accord with the limit derived in Ref. 6 (where the ND rate was used). Given the overall uncertainties in deriving these axion mass limits (see Refs. 6–8 for discussion of the uncertainties), there now seems to be reasonable agreement that the axion mass limit based upon SN1987A is $m_a \lesssim 10^{-3}$ eV.

Finally, we mention some work in progress.[14] In order to obtain a reliable limit to the axion mass based upon axion emission from SN1987A one needs to compare the theoretical predictions of collapse calculations which incorporate axions in a self-consistent way[15] to the observables at hand. In this case "the observables" are the neutrino events detected by Irvine-Brookhaven-Michigan (IMB) and Kamiokande (KII) water Cherenkov detectors.[16] We have recently added axion cooling to postcollapse models of SN1987A, and computed the neutrino signals expected in the KII and IMB detectors.[14] As expected, the duration of the neutrino burst proves to be very sensitive to the axion mass. For $m_a \gtrsim 10^{-3}$ eV, the length of the neutrino pulse drops precipitously from ~ 9 sec to less than 4 sec for KII, and from ~ 4 sec to less than 2 sec for IMB, strongly suggesting that an axion mass $\gtrsim 10^{-3}$ eV is inconsistent with the neutrino observations of SN1987A.

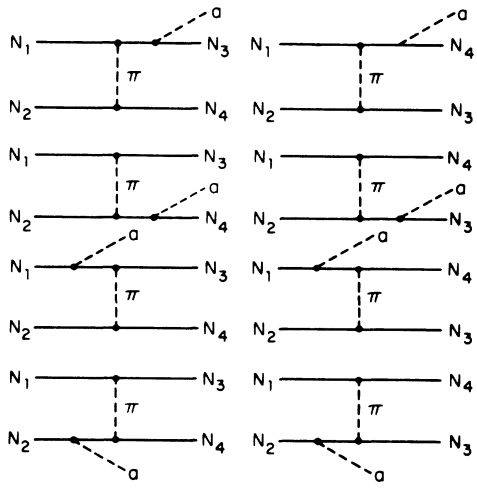

FIG. 4. The direct and exchange diagrams for nucleon, nucleon axion bremsstrahlung. From top left to bottom left the direct diagrams are referred to as a, b, c, d; and from top right to bottom right the exchange diagrams are referred to as a',b',c',d'.

ACKNOWLEDGMENTS

We gratefully acknowledge the suggestion of E.W. Kolb which stimulated this work, and useful conversations with E.W. Kolb, G. Steigman, and J.N. Fry. We also thank H.-S. Kang for checking our calculation of $|\mathcal{M}|^2$ and for pointing out several errors therein. This work was supported in part by the DOE (at Chicago and Fermilab), NASA (at Fermilab), The German National Scholarship Foundation (R.P.B.), and The Alfred P. Sloan Foundation (M.S.T.).

APPENDIX

Here we discuss the matrix element squared $|\mathcal{M}|^2$ for the three bremsstrahlung processes $n+n \to n+n+a$, $p+p \to p+p+a$, and $n+p \to n+p+a$, and provide the expression for the total axion emission rate from all three processes. In the one-pion-exchange (OPE) approximation there are four direct and four exchange diagrams, corresponding to the axion being emitted by any one of the four nucleons (see Fig. 4). Iwamoto[10] has calculated $|\mathcal{M}|^2$ for the process $n+n \to n+n+a$ in the degenerate limit; he obtains

$$\sum_{\text{spin}} |\mathcal{M}|^2 = \frac{256}{3} \frac{g_{an}^2 f^4 m^2}{m_\pi^4} \left[\frac{|\mathbf{k}|^4}{(|\mathbf{k}|^2+m_\pi^2)^2} + \frac{|l|^4}{(|l|^2+m_\pi^2)^2} + \frac{|\mathbf{k}|^2|l|^2}{(|\mathbf{k}|^2+m_\pi^2)(|l|+m_\pi^2)} \right],$$

where $f \simeq 1.05$ is the pion-neutron coupling, g_{an} is the axion-neutron coupling, and $k=p_2-p_4$, $l=p_2-p_3$. In the limit of interest, $3mT \gg m_\pi^2$ and $|\mathbf{k}|^2$, $|l|^2 \sim 3mT \gg m_\pi^2$, so that the quantity in large parentheses is very nearly 3.

All together there are 64 diagrams which contribute to each matrix element squared. We have explicitly calculated and summed up all 64 terms for the three bremsstrahlung processes. We will briefly describe our computations. The momenta of the four nucleons are denoted by p_1,p_2,p_3,p_4 and that of the axion by a; in addition, the momentum transfer for the direct diagrams is $k=p_2-p_4$ and for the exchange diagrams, $l=p_2-p_3$. To lowest order in T/m, $k^2 \simeq -|\mathbf{k}|^2$ and $l^2 \simeq -|l|^2$. The pion-nucleon coupling is $(2m/m_\pi) f_{ij} \gamma_5$, where $f_{nn}=f$, $f_{pp}=-f$, $f_{pn}=\sqrt{2}f$ (as required by isospin invariance). For the nn and pp processes there is a relative minus sign between the direct and exchange diagrams because of the interchange of identical fermions. The axion-nucleon coupling is $(g_{ai}/2m)\gamma_5 \not{a}$, where $g_{ai}=g_{an}$ (i=neutron) or g_{ap} (i=proton).[17] Of the 64 diagrams only 48 are nonzero, and these can be grouped into four categories which we will now discuss in more detail. Here and throughout we refer to the diagrams by their labels a, b, c, d, and a', b', c', d'.

(i) $|a|^2$, $|b|^2$, $|c|^2$, $|d|^2$, $|a'|^2$, $|b'|^2$, $|c'|^2$, $|d'|^2$. The prototype calculation is that, for $|a|^2$,

$$\sum_{\text{spin}} |a|^2 = \frac{4g_{a3}^2 f_{13}^2 f_{24}^2 m^2}{m_\pi^4} \frac{1}{(k^2-m_\pi^2)^2} \frac{1}{(p_3\cdot a)^2} \mathrm{Tr}(\not{p}_3+m)(p_3\cdot a - m\not{a})(\not{p}_1+m)(p_3\cdot a - m\not{a})\mathrm{Tr}(\not{p}_4+m)(\not{p}_2-m)$$

$$= 16 \frac{g_{a3}^2 f_{13}^2 f_{24}^2 m^2}{m_\pi^4} \frac{|\mathbf{k}|^4}{(|\mathbf{k}|^2+m_\pi^2)^2},$$

where we have kept only terms to lowest order in T/m.

(ii) $(a\cdot c^*+c\cdot a^*)$, $(d\cdot b^*+b\cdot d^*)$, $(a'\cdot c'^*+c'\cdot a'^*)$, $(d'\cdot b'^*+b'\cdot d'^*)$. The prototype for these diagrams is the interference between diagrams a and c:

$$\sum_{\text{spin}}(a\cdot c^*+c\cdot a^*)=\frac{8g_{a1}g_{a3}f_{13}^2f_{24}^2m^2}{m_\pi^4}\frac{1}{p_1\cdot ap_3\cdot a}\frac{1}{(k^2-m_\pi^2)^2}\mathrm{Tr}(\not p_4+m)(\not p_2-m)$$
$$\times\mathrm{Tr}(\not p_3+m)(p_1\cdot a-m\not a)(\not p_1+m)(p_3\cdot a-m\not a)$$
$$=\frac{32g_{a1}g_{a3}f_{13}^2f_{24}^2m^2}{m_\pi^4}\left[1+\frac{2m^2(k\cdot a)^2}{k^2p_1\cdot ap_2\cdot a}\right]\frac{|\mathbf{k}|^4}{(|\mathbf{k}|^2+m_\pi^2)^2}$$
$$=\frac{32g_{a1}g_{a3}f_{13}^2f_{24}^2m^2}{3m_\pi^4}\frac{|\mathbf{k}|^4}{(|\mathbf{k}|^2+m_\pi^2)^2},$$

where the final form follows from averaging over the direction of the axion: $\langle(\hat{\mathbf{k}}\cdot\hat{\mathbf{a}})^2\rangle=\frac{1}{3}$.

(iii) $(a\cdot b'^*+b'\cdot a^*)$, $(c\cdot c'^*+c'\cdot c^*)$, $(d\cdot d'^*+d'\cdot d^*)$, $(b\cdot a'^*+a'\cdot b^*)$. The prototype for these diagrams is the interference between diagrams c and c':

$$\sum_{\text{spin}}(c\cdot c'^*+c'c^*)=\frac{8g_{a1}^2f_{13}f_{14}f_{24}f_{23}m^2}{m_\pi^4}\frac{1}{(l^2-m_\pi^2)}\frac{1}{(k^2-m_\pi^2)}\mathrm{Tr}(\not p_3+m)(\not p_1-m)(\not p_4+m)(\not p_2-m)$$
$$=\frac{-16g_{a1}^2f_{13}f_{14}f_{24}f_{23}m^2}{m_\pi^4}\frac{|\mathbf{k}|^2|\boldsymbol{l}|^2-2(k\cdot l)^2}{(|\boldsymbol{l}|^2+m_\pi^2)(|\mathbf{k}|^2+m_\pi^2)}.$$

Remember for the pp and nn processes an additional factor of (-1) must be in included because of the relative minus sign between the direct and exchange diagrams.

(iv)

$(a\cdot a'^*+a'\cdot a^*)$, $(a\cdot c'^*+c'\cdot a^*)$, $(a\cdot d'^*+d'\cdot a^*)$;

$(c\cdot a'^*+a'\cdot c^*)$, $(c\cdot d'^*+d'\cdot c^*)$, $(c\cdot b'^*+b'\cdot c^*)$;

$(d\cdot a'^*+a'\cdot d^*)$, $(d\cdot c'^*+c'\cdot d^*)$, $(d\cdot b'^*+b'\cdot d^*)$;

$(b\cdot c'^*+c'\cdot b^*)$, $(b\cdot d'^*+d'\cdot b^*)$, $(b\cdot b'^*+b'\cdot b^*)$.

These diagrams are by far the most challenging to evaluate. The prototype calculations are for $(a\cdot a'^*+a'\cdot a^*)$, $(a\cdot c'^*+c'\cdot a^*)$, and $(a\cdot d'^*+d'\cdot a^*)$:

$$\sum_{\text{spin}}(a\cdot a'^*+a'\cdot a^*)=\frac{16g^2f^4m^2}{m_\pi^4}\frac{1}{(k^2-m_\pi^2)}\frac{1}{(l^2-m_\pi^2)}\left[-k^2l^2+2(k\cdot l)^2-\frac{2m^2k^2(l\cdot a)^2}{(p\cdot a)^2}-\frac{2m^2l^2(k\cdot a)^2}{(p\cdot a)^2}+\frac{4m^2(k\cdot l)(k\cdot a)(l\cdot a)}{(p\cdot a)^2}\right]$$
$$=\frac{3+2\beta}{9}\frac{16g^2f^4m^2}{m_\pi^4}\frac{|\mathbf{k}|^2|\boldsymbol{l}|^2}{(|\mathbf{k}|^2+m_\pi^2)(|\boldsymbol{l}|^2+m_\pi^2)},$$

$$\sum_{\text{spin}}(a\cdot c'^*+c'\cdot a^*)=\frac{16g^2f^4m^2}{m_\pi^4}\frac{1}{(k^2-m_\pi^2)}\frac{1}{(l^2-m_\pi^2)}\left[-k^2l^2+2(k\cdot l)^2-\frac{2m^2l^2(k\cdot a)^2}{(p\cdot a)^2}+\frac{4m^2(k\cdot l)(k\cdot a)(l\cdot a)}{(p\cdot a)^2}\right]$$
$$=-\frac{3-2\beta}{9}\frac{16g^2f^4m^2}{m_\pi^4}\frac{|\mathbf{k}|^2|\boldsymbol{l}|^2}{(|\mathbf{k}|^2+m_\pi^2)(|\boldsymbol{l}|^2+m_\pi^2)},$$

$$\sum_{\text{spin}}(a\cdot d'^*+d'\cdot a^*)=\frac{16g^2f^4m^2}{m_\pi^4}\frac{1}{(k^2-m_\pi^2)}\frac{1}{(l^2-m_\pi^2)}\left[-k^2l^2+2(k\cdot l)^2-\frac{2m^2k^2(l\cdot a)^2}{(p\cdot a)^2}+\frac{4m^2(k\cdot l)(k\cdot a)(l\cdot a)}{(p\cdot a)^2}\right]$$
$$=-\frac{3-2\beta}{9}\frac{16g^2f^4m^2}{m_\pi^4}\frac{|\mathbf{k}|^2|\boldsymbol{l}|^2}{(|\mathbf{k}|^2+m_\pi^2)(|\boldsymbol{l}|^2+m_\pi^2)},$$

where the final expressions follow from averaging over the direction of the axion: $\langle(\hat{\mathbf{k}}\cdot\hat{\mathbf{a}})^2\rangle=\frac{1}{3}$ and $\langle(\hat{\mathbf{k}}\cdot\hat{\mathbf{a}})(\hat{\boldsymbol{l}}\cdot\hat{\mathbf{a}})(\hat{\mathbf{k}}\cdot\hat{\boldsymbol{l}})\rangle=\frac{1}{3}(\hat{\mathbf{k}}\cdot\hat{\boldsymbol{l}})^2$. There are kinematical constraints on the quantity $\hat{\mathbf{k}}\cdot\hat{\boldsymbol{l}}$, so that $\langle(\hat{\mathbf{k}}\cdot\hat{\boldsymbol{l}})^2\rangle$ is not necessarily equal to $\frac{1}{3}$. We define $\langle(\hat{\mathbf{k}}\cdot\hat{\boldsymbol{l}})^2\rangle\equiv\beta/3$; in the degenerate limit kinematics require that $\beta=0$. In the nondegenerate limit

$$\langle(\hat{\mathbf{k}}\cdot\hat{\mathbf{l}})^2\rangle=\tfrac{105}{16}\int_0^1\frac{x(1-x^2)^4}{(1+x^2)^2}\ln\left|\frac{1+x}{1-x}\right|dx\simeq\frac{1.0845}{3}$$

so that $\beta(\mathrm{ND})\rightarrow 1.0845$. For simplicity the indicies on g_{ai} and f_{ij} have been suppressed. Remember that for the pp and nn processes an additional factor of (-1) must be included.

(v)

$$(a\cdot d^*+d\cdot a^*),\ (a\cdot b^*+b\cdot a^*),\ (c\cdot d^*+d\cdot c^*),$$
$$(c\cdot b^*+b\cdot c^*),\ (a'\cdot d'^*+d'\cdot a'^*),\ (a'\cdot b'^*+b'\cdot a'^*),$$
$$(c'\cdot d'^*+d'\cdot c'^*),\ (c'\cdot b'^*+b'\cdot c'^*).$$

All of these interference terms vanish as they are proportional to

$$\mathrm{Tr}(\not p+m)(p\cdot a-m\not a)(\not p+m)\gamma_5\mathrm{Tr}(\not p+m)\gamma_5(\not p+m)(p\cdot a-m\not a).$$

Summing all the diagrams, we obtain, for $n+n\rightarrow n+n+a$,

$$\sum_{\text{spin}}|\mathcal{M}|^2=\frac{256}{3}\frac{g_{an}^2f^4m^2}{m_\pi^4}\left[\frac{|\mathbf{k}|^4}{(|\mathbf{k}|^2+m_\pi^2)^2}+\frac{|\mathbf{l}|^4}{(|\mathbf{l}|^2+m_\pi^2)^2}+\frac{(1-\beta)|\mathbf{k}|^2|\mathbf{l}|^2}{(|\mathbf{k}|^2+m_\pi^2)(|\mathbf{l}|^2+m_\pi^2)}\right]$$

and, for $p+p\rightarrow p+p+a$,

$$\sum_{\text{spin}}|\mathcal{M}|^2=\frac{256}{3}\frac{g_{ap}^2f^4m^2}{m_\pi^4}\left[\frac{|\mathbf{k}|^4}{(|\mathbf{k}|^2+m_\pi^2)^2}+\frac{|\mathbf{l}|^4}{(|\mathbf{l}|^2+m_\pi^2)^2}+\frac{(1-\beta)|\mathbf{k}|^2|\mathbf{l}|^2}{(|\mathbf{k}|^2+m_\pi^2)(|\mathbf{l}|^2+m_\pi^2)}\right].$$

In the degenerate limit $\beta=0$, and our result agrees with that of Iwamoto.[10] For $n+p\rightarrow n+p+a$ we obtain

$$\sum_{\text{spin}}|\mathcal{M}|^2=\frac{256f^4m^2}{3m_\pi^4}\frac{(g_{an}+g_{ap})^2}{4}\left[\frac{2|\mathbf{l}|^4}{(|\mathbf{l}|^2+m_\pi^2)^2}-\frac{4\beta}{3}\frac{|\mathbf{k}|^2|\mathbf{l}|^2}{(|\mathbf{l}|^2+m_\pi^2)(|\mathbf{k}|^2+m_\pi^2)}\right]$$
$$+\frac{256f^4m^2}{3m_\pi^4}\frac{g_{an}^2+g_{ap}^2}{2}\left[\frac{|\mathbf{k}|^4}{(|\mathbf{k}|^2+m_\pi^2)^2}+\frac{2(3-\beta)}{3}\frac{|\mathbf{k}|^2|\mathbf{l}|^2}{(|\mathbf{l}|^2+m_\pi^2)(|\mathbf{k}|^2+m_\pi^2)}+2\frac{|\mathbf{l}|^4}{(|\mathbf{l}|^2+m_\pi^2)^2}\right].$$

For $g_{an}=g_{ap}$ and $|\mathbf{l}|^2$, $|\mathbf{k}|^2\gg m_\pi^2$, this result is a factor of $(7-2\beta)/(3-\beta)$ times that for $n+n\rightarrow n+n+a$ or $p+p\rightarrow p+p+a$.

In order to make our calculation of the axion emission rate tractable we have neglected the momentum dependence of $|\mathcal{M}|^2$. In the degenerate regime Iwamoto has included the momentum dependence of $|\mathcal{M}|^2$ in his calculation:[10] it leads to a factor of $F(x)=1-\frac{3}{2}x\arctan(x^{-1})+x^2/2(1+x^2)$ multiplying his rates [$x\equiv m_x/2p_F(n)$]. For the density of interest, $X_n\rho=4\times10^{14}\mathrm{g\,cm^{-3}}$, this reduction factor is $F\simeq0.64$. We can estimate the effect of the momentum dependence on our rates. The momentum dependence of $|\mathcal{M}|^2$ appears in the form of factors such as $|\mathbf{q}|^4/(|\mathbf{q}|^2+m_\pi^2)^2$. Taking $|\mathbf{q}|^2\sim3mT$, this factor is 0.86($T=80$ MeV), 0.81(60 MeV), 0.74(40 MeV), 0.57(20 MeV), and 0.37(10 MeV). With this fact in mind we take $|\mathcal{M}|^2$ to be constant.

Making this approximation it is straightforward to write down the total axion emission rate, from all three processes:

$$\dot{\epsilon}_a=64(m^{2.5}T^{6.5}/m_\pi^4)f^4\left[(1-\beta/3)g_{an}^2I(y_1,y_1)+(1-\beta/3)g_{ap}^2I(y_2,y_2)+\frac{4(15-2\beta)}{9}\left[\frac{g_{an}^2+g_{ap}^2}{2}\right]I(y_1,y_2)\right.$$
$$\left.+\frac{4(6-4\beta)}{9}\left[\frac{g_{an}+g_{ap}}{2}\right]^2I(y_1,y_2)\right],\qquad\text{(A1)}$$

where the first term accounts for $n+n\rightarrow n+n+a$, the second term for $p+p\rightarrow p+p+a$, and the third and fourth terms for $n+p\rightarrow n+p+a$. $I(y_1,y_2)$ is as defined in Eq. (8); also note, that as defined, $I(y,y)=I(y)$, where $I(y)$ is defined in Eq. (7). For reference, $64m^{2.5}T^{6.5}m_\pi^{-4}f^4=1.66\times10^{48}$ erg cm^{-3}sec$^{-1}f^4T_{\mathrm{MeV}}^{6.5}$. Note that $\beta\equiv3\langle(\hat{\mathbf{k}}\cdot\hat{\mathbf{l}})^2\rangle$ depends upon the level of degeneracy; for very degenerate conditions $\beta=0$; while for nondegenerate conditions $\beta=1.0845$. Taking for the moment $g_{an}=g_{ap}$ and $y_1=y_2$, we see that the pn bremsstrahlung process is a factor of $4(7-2\beta)/(3-\beta)$ ($=\frac{28}{3}$ for $\beta=0$; $=10$ for $\beta=1$) more important than either the nn or pn processes. The factor of 4 traces to the absence of the statistical factor of $\frac{1}{4}$ for identical particles in the initial and final states; and the factor of $(7-2\beta)/(3-\beta)$ traces to the stronger coupling of charged pions to nucleons.

From this expression the effective axion-nucleon cou-

pling for the *pn* process, defined just below Eq. (9), can easily be read off:

$$g_{aN}^2 = \frac{15-2\beta}{9}\left[\frac{g_{an}^2+g_{ap}^2}{2}\right]+\frac{6-4\beta}{9}\left[\frac{g_{an}+g_{ap}}{2}\right]^2 .$$

Given that $f\sim 1$, the validity of the one-pion-exchange approximation is open to question: what about the inclusion of two-pion, three-pion,..., exchange, other meson-exchange diagrams, collective nuclear effects, etc.? We will not address these issues here.

[1]G.'t Hooft, Phys. Rev. Lett. **37**, 8 (1976); R. D. Peccei and H. R. Quinn, *ibid.* **38**, 1440 (1977); F. Wilczek, *ibid.* **40**, 279 (1978); S. Weinberg, *ibid.* **40**, 223 (1978); M. Dine, W. Fischler, and M. Srednicki, Phys. Lett. **104B**, 199 (1981); A. R. Zhitnitsky, Yad. Fiz. **31**, 497 (1980) [Sov. J. Nucl. Phys. **31**, 260 (1980)]; J. Kim, Phys. Rev. Lett. **43**, 103 (1979); M. Shifman, A. Vainshtein, and V. Zakharov, Nucl. Phys. **B166**, 493 (1980).

[2]D. Kaplan, Nucl. Phys. **B260**, 215 (1985); P. Sikivie, in *Cosmology and Particle Physics,* edited by E. Alvarez *et al.* (World Scientific, Singapore, 1987), p. 144.

[3]M. Srednicki, Nucl. Phys. **B260**, 689 (1985).

[4]See, e.g., J.-E. Kim, Phys. Rep. **150**, 1 (1987); H.-Y. Cheng, *ibid.* **158**, 1 (1988); or, L. L. Krauss, in *High Energy Physics 1985,* edited by M. Bowick and F. Gursey (World Scientific, Singapore, 1986).

[5]J. Preskill, M. Wise, and F. Wilczek, Phys. Lett. **120B**, 127 (1983); L. Abbott and P. Sikivie, *ibid.* **120B**, 133 (1983); M. Dine and W. Fischler, *ibid.* **120B**, 137 (1983). The limit quoted here is from M. S. Turner, Phys. Rev. D **33**, 889 (1986); if the Universe inflated before or during Peccei-Quinn spontaneous symmetry breaking, the limit depends upon the initial misalignment angle to the 1.7 power. If the Universe never underwent inflation, then axion production by the decay of axionic strings may also be a significant source of axions, and may lead to a more stringent lower bound to m_a. See R. L. Davis, Phys. Lett. B **180**, 225 (1986); D. Harari and P. Sikivie, *ibid.* **195**, 361 (1987).

[6]M. S. Turner, Phys. Rev. Lett. **60**, 1797 (1988). Here it is also shown that for axion masses $\gtrsim 0.02$ eV axion reabsorption is important, and that for $m_a \gtrsim 2.2$ eV reabsorption reduces axion emission to the extent that such an axion is not precluded by SN1987A.

[7]R. Mayle *et al.*, Phys. Lett. B **203**, 188 (1988).

[8]G. G. Raffelt and D. Seckel, Phys. Rev. Lett. **60**, 1793 (1988).

[9]See, e.g., H. A. Bethe *et al.*, Nucl. Phys. **A324**, 487 (1979); J. M. Lattimer *et al.*, *ibid.* **A432**, 646 (1985); A. Burrows and J. M. Lattimer, Astrophys. J. **307**, 178 (1986); W. Hillebrandt, Ann. N.Y. Acad. Sci. **422**, 197 (1984); J. Wilson, in *Numerical Astrophysics,* edited by J. Centrella *et al.* (Jones & Bartlett, Boston, 1984).

[10]N. Iwamoto, Phys. Rev. Lett. **53**, 1198 (1984). In quoting Iwamoto's axion emission rate, we have corrected it for a forgotten factor of 2 (for identical particles in the initial state).

[11]Mayle *et al.* (see Ref. 7) have also computed $\dot{\epsilon}_a$(ND). However their rate has the wrong temperature dependence: $\dot{\epsilon}_a$(ND, Mayle *et al.*) $\simeq 3.5\times 10^{48}$ erg cm^{-3} sec$^{-1} f^4 g_{an}^2 (X_n\rho_{14})^2 T_{\rm MeV}^3$, corresponding to $\epsilon_a \propto T^6 F(y)$, cf. Eq. (4) and below. We have taken the liberty of correcting the ND emission rate computed in Ref. 6 for a factor of 2 algebra error.

[12]The limits derived in Ref. 8 cannot be easily compared to those of Refs. 6 and 7, as the authors of Ref. 8 do not explicitly specify the relationship between the axion-nucleon coupling and the axion mass. However, if one infers that relationship, their bound is comparable to that of Ref. 6.

[13]In obtaining Eq. (5c), the expression for axion emission in the ND limit in terms of ρ, X_n, and T, we have used the relationship $e^y \simeq 125 X_n \rho_{14} T_{\rm MeV}^{-3/2}$, which is valid only in the ND limit ($y \ll -1$). One might have been tempted to use the exact expression for y, obtained by solving $g(y)=111 X_n \rho_{14} T_{\rm MeV}^{-3/2}$, where $g(y)=\int_0^\infty u^{1/2} du/(e^{u-y}+1)$. In addition to the obvious fact that $\dot{\epsilon}_a$(ND) then could not be written in closed form (except for $y \ll -1$), the resulting expression when extrapolated to $y \gtrsim 0$ gives a larger value for $\dot{\epsilon}_a$(ND) which overestimates the true emission rate by a larger factor than Eq. (5c) and does not even decrease monotonically with decreasing temperature (increasing y). The simple limiting form chosen in Eq. (5c) extrapolates to the semidegenerate regime much better, and of course has the same form in the very nondegenerate regime.

[14]A. Burrows, R. P. Brinkmann, and M. S. Turner, Fermilab Report No. Pub-88/105A, 1988 (unpublished).

[15]Collapse models without axion emission (see, e.g., Ref. 9) indicate postcollapse, central temperatures of order 30–80 MeV. When the effect of axion cooling is self-consistently taken into account, the central core temperature will drop, thereby quenching axion emission. It is necessary to take this into account properly to obtain a reliable limit to the axion mass. The first steps toward this end were taken in Refs. 7 and 8.

[16]K. Hirata *et al.*, Phys. Rev. Lett. **58**, 1490 (1987); R. M. Bionta *et al.*, *ibid.* **58**, 1494 (1987).

[17]Both the axion and pion are Nambu-Goldstone bosons, and fundamentally have derivative (pseudovector) couplings: axion, $(g_{ai}/2m)\gamma_5\gamma_\mu$; pion $(f/m_\pi)\gamma_5\gamma_\mu$. By appropriate phase rotations of the nucleon fields their derivative couplings can be made to be pseudoscalar couplings: axion, $g_{ai}\gamma_5$; pion, $f(2m/m_\pi)\gamma_5$. However, both the axion and pion couplings cannot simultaneously be made pseudoscalar without the introduction of additional contact terms (as also noted in Ref. 8): without additional contact terms only one coupling can be made pseudoscalar. This explains the discrepancy between Iwamoto's work and that of A. Pantziris and K. Kang [Phys. Rev. D **33**, 3509 (1986)], who also calculated the matrix element squared for $n+n\rightarrow n+n+a$, and obtained a result that is a factor of (m/T) larger than that of Iwamoto. Iwamoto used a pseudoscalar coupling for the axion and a pseudovector coupling for the pion, while Pantziris and Kang used pseudoscalar couplings for both, and neglected the required contact terms.